Vacuum 82 (2008) 1177–1182

Contents lists available at ScienceDirect

Vacuum

journal homepage: www.elsevier.com/locate/vacuum

Relational analysis between parameters and defects for electron beam welding of AZ-series magnesium alloys

Chao-Ting Chi [a,*], Chuen-Guang Chao [b], Tzeng-Feng Liu [b], Che-Chung Wang [c]

[a] System Manufacturing Center, Chung-Shan Institute of Science and Technology, P.O. Box 90008-14, Sanxia 237, Taipei, Taiwan, Republic of China
[b] Department of Materials Science and Engineering, National Chiao Tung University, Hsinchu 300, Taiwan, Republic of China
[c] Graduate School of Industrial Design and Architecture, Shih-Chien University, Taipei 104, Taiwan, Republic of China

ARTICLE INFO

Article history:
Received 19 April 2007
Received in revised form 19 November 2007
Accepted 14 December 2007

Keywords:
Magnesium alloy
Electron beam welding
Taguchi's method
Grey relational analysis

ABSTRACT

In the last half century, lightweight magnesium alloy has gradually shifted from military applications to civil applications. More noteworthy is that its low melting point, high thermal conductivity, and superior fluidity are good for weld pool flow and welding parameter research. This paper presents a novel approach to these characteristics, which analyzes the influences of electron beam welding parameters on weldment strength and defect formation by linking Taguchi's method with the grey relational analysis. Not only are the parameter contribution and the defect weight individually quantified, but also the relationship between welding parameters and defect dimensions can also be obtained this way.

1. Introduction

Created in the 1950s, electron beam welding (EBW) has been improved many times during the last several decades. It has become the best welding technology to date, displaying superior performance regardless of the input power, power supply, operational environment or welding precision [1]. EBW focuses electrons at a high speed, impacting the work piece. This collision immediately transforms kinetic energy into thermal energy, and then forms a keyhole containing melting and evaporating material [2]. As the electron beam moves forward, the melting and evaporating material flows from the front to the rear of the keyhole. This process forms a weld with high depth-to-width ratio using the interaction between high energy density and local vapor pressure [3]. Thus, the optimal design of parameters and proper choice of material are important for the successful application of EBW processes.

When all EBW parameters (i.e. acceleration voltage, beam current, welding speed, focal position, etc.) match each other, the electron beam energy can form a symmetrical Gaussian distribution [4,5], which further influences the relationship between the electron beam's force of impact, the electromagnetic force, the repulsive force of the evaporating material, the surface tension force, and gravity in the weld [6]. In other words, the weldment strength, weld width, penetrating depth, and thermal transfer efficiency can be changed by using different material [7–12]. Welding a material with high thermal conductivity under a high vacuum greatly reduces many harmful influences such as oxidation and heat-affected zones. Further, parameter characteristics are easily revealed from superior fluidity and high vapor pressure as welding a material with a low melting and boiling point. Based on these factors, magnesium alloy (vapor without toxicity) is the best choice of all engineering materials.

Many parameters must be set to control an EBW machine. Testing the possible parameters by trial and error, or changing one factor at a time, can waste a lot of time and money. A previous study [12] uses Taguchi's method to precisely predict the infeasible data and the optimum parameters for the EBW of AZ-series magnesium alloys (AZ31B, AZ61A, and AZ91D) and obtains the effect of each parameter by analysis of variance (ANOVA) and contribution. These findings enable great savings in cost and time. This study integrates and further discusses the EBW of AZ-series alloy, revealing that material differences are one of the control parameters necessary to understand the influence of Al content. However, Taguchi's method cannot handle problems with multiple performance characteristics such as the relationship between welding parameters and weld defects (e.g. undercut, root concavity, crack, cavity, and pore). This lack indicates a need for the following additional design refinement.

Dr. Deng first proposed grey relational analysis in 1982, meeting the crucial mathematical criteria for dealing with poor, incomplete, and uncertain systems [13,14]. Grey relational analysis can be used to effectively solve the complicated interrelationships between

* Corresponding author. Tel.: +886 916 930 630.
E-mail addresses: joseph.mse92g@nctu.edu.tw (C.-T. Chi), c_g_chao@hotmail.com (C.-G. Chao), coe@cc.nctu.edu.tw (T.-F. Liu), zcwang@mail.usc.edu.tw (C.-C. Wang).

0042-207X/$ – see front matter
doi:10.1016/j.vacuum.2007.12.019

multiple performance characteristics [15–17]. As its name implies, grey relational analysis exhibits infinite possibilities between black and white (or 1 and 0). Depending on the quality characteristics chosen, the measured data can be normalized ($0 \le x_{ij} \le 1$) using a "higher-the-better" (HB), "lower-the-better" (LB), or "nominal-the-better" (NB) criterion. These criterions are expressed as follows:

$$\mathrm{HB}: x_{ij} = \frac{y_{ij} - \min\limits_j y_{ij}}{\max\limits_j y_{ij} - \min\limits_j y_{ij}} \tag{1}$$

$$\mathrm{LB}: x_{ij} = \frac{\max\limits_j y_{ij} - y_{ij}}{\max\limits_j y_{ij} - \min\limits_j y_{ij}} \tag{2}$$

$$\mathrm{NB}: x_{ij} = 1 - \frac{\left|y_{ij} - y\right|}{\max\left\{\max\limits_j y_{ij} - y_{ij}; y_{ij} - \min\limits_j y_{ij}\right\}} \tag{3}$$

where y_{ij} is the original sequence for the ith experimental result in the jth performance characteristic, y is the assigned value, and max y_{ij} and min y_{ij} are the maximum and minimum values in the original sequence, respectively.

When x_i^0 and x_{ij} are the reference sequence and the comparability sequence, respectively, the grey relational coefficient (γ_{ij}) can be defined as:

$$\gamma_{ij} = \frac{\min\limits_i \min\limits_j |x_i^0 - x_{ij}| + \zeta \max\limits_i \max\limits_j |x_i^0 - x_{ij}|}{|x_i^0 - x_{ij}| + \zeta \max\limits_i \max\limits_j |x_i^0 - x_{ij}|} \tag{4}$$

where ζ is the distinguishing coefficient ($0 \le \zeta \le 1$) which can be adjusted in accordance with the actual condition. The average grey relational coefficient is the grey relational grade. Because each performance characteristic may influence the system differently, the grey relational grade ($0 < \gamma_j^* \le 1$) can be modified by weights and expressed as:

$$\gamma_j^* = \sum_{i=1}^{n} \gamma_{ij} \omega_i \tag{5}$$

The weight ($\omega_i, \Sigma\omega_i = 1$) of each performance characteristic can be set using the assigned method or entropy method. The latter is used when researchers cannot determine which performance characteristic is more important. Therefore, the entropy (E_i), relative weight (λ_i) and entropy weight ($\omega_{ei}, \Sigma\omega_{ei} = 1$) of each performance characteristic are defined as:

$$E_i = \frac{1}{0.6487m} \sum_{j=1}^{m} W_e\left(\frac{x_{ij}}{\sum_{j=1}^{m} x_{ij}}\right) \tag{6}$$

$$W_e(x) \equiv x e^{(1-x)} + (1-x)e^x - 1 \tag{7}$$

$$\lambda_i = \frac{(1 - E_i)}{n - \sum_{i=1}^{n} E_i} \tag{8}$$

$$\omega_{ei} = \frac{\lambda_i}{\sum_{i=1}^{n} \lambda_i} \tag{9}$$

Both Taguchi's method and grey relational analysis have been separately applied to various studies [12,18–20], but only a few publications in recent years have paired both methods together to study the relationship between laser welding parameters and the mechanical properties of titanium alloy weldment [15–17]. To further explore the core question of this paper, the authors used EBW of AZ-series alloys with both statistical analyzes to better understand the relationship between welding parameters, weldment strength, and weld defects.

Table 1
Factors and levels in the experimental design for the EBW machine[a]

Code	Parameter (unit)	Levels			Observed value
		1	2	3	
A	Stress relief	No	Yes	–	UTS
B	Accelerating voltage (kV)	100	110	120	
C	Beam current (mA)	20	25	30	
D	Welding speed (mm/s)	30	40	50	
E	Focal position (mm)	0	11	22	
F	Radius of oscillated EB (mm)	0	0.1	0.2	
G	Frequency of oscillated EB (Hz)	0	100	200	
H	Material difference (Al content)	AZ31B	AZ61A	AZ91D	

[a] The condition used for stress relief was 260 °C for 15 min after welding (within 24 h). The focal position, which is within the interval of the plate thickness, is referred to the surface of the work piece (0), and the positive direction is downward.

2. Experimental method

Home-made AZ31B, AZ61A, and AZ91D extruded plates with dimensions of $105 \times 60 \times 12$ mm^3 were used in our experiments. A 0.5-mm thick layer was removed from the outside of these plates around the weld area to prevent the oxide layer from affecting the results. These work pieces were cleaned by acetone, reserved in a vacuum desiccator (0.133 Pa), and then welded together under high vacuum (0.004 Pa) by a butting process without filler in a work chamber. The resulting weldment dimension was $104 \times 119 \times 11$ mm^3.

The weldment tensile properties were precisely analyzed according to the following. Welds at the halfway point along the gage length in standard tensile specimens were perpendicular to the longitudinal direction. These weldments were then cut into one metallographic ($15 \times 10 \times 11$ mm^3) specimen and six tensile specimens (according to the subsize specimen in ASTM B557-02 standard inspection [21]) along the extruded direction. After the tensile test, the influences of EBW parameters on the weldment strength were analyzed by Taguchi's method to obtain the optimum parameters, analysis of variance, and contribution. Table 1 shows the experimental design using this $L_{18}(2^1 \times 3^7)$ orthogonal array, including the levels of each factor. Computer software (Image-Pro Plus 6.0) then precisely measured various defect dimensions, which were treated by grey relational analysis in accordance with the metallographic weld cross-section photograph. The weights of dimensions and defects were adjusted with the aim of changing the order of integrated data and matching it with the order of weldment strength as closely as possible. The terminal weights were multiplied by the EBW parameter contribution, and the product was the affected extent of various defects on each parameter. Thus calculated, the affected extent of defect dimensions on each parameter was also obtained.

Table 2
Chemical composition for AZ-series alloys [wt.%]

Materials	Element				
	Mg (Cu)	Al (Fe)	Zn (P)	Mn (Pb)	Si (Be)
AZ31B	96.2467 (0.0004)	2.8150 (0.0025)	0.6395 (0.0013)	0.2835 (0.0008)	0.0094 (0.0009)
AZ61A	93.0585 (0.0007)	5.8800 (0.0030)	0.7985 (0.0012)	0.2205 (0.0062)	0.0240 (–)
AZ91D	90.3148 (0.0012)	8.8550 (0.0041)	0.5474 (0.0012)	0.2600 (0.0017)	0.0143 (0.0003)

Table 3
S/N ratios (η) of UTS of weldments for HV-EBW of AZ-series alloys

No.	Parameters and levels								S/N ratio of UTS (dB)
	A	B	C	D	E	F	G	H	
1	1	1	1	1	1	1	1	1	44.71
2	1	1	2	2	2	2	2	2	45.79
3	1	1	3	3	3	3	3	3	44.25
4	1	2	1	1	2	2	3	3	47.79
5	1	2	2	2	3	3	1	1	42.91
6	1	2	3	3	1	1	2	2	42.93
7	1	3	1	2	1	3	2	3	41.90
8	1	3	2	3	2	1	3	1	45.30
9	1	3	3	1	3	2	1	2	47.82
10	2	1	1	3	3	2	2	1	36.27
11	2	1	2	1	1	3	3	2	42.85
12	2	1	3	2	2	1	1	3	48.56
13	2	2	1	2	3	1	3	2	45.75
14	2	2	2	3	1	2	1	3	45.05
15	2	2	3	1	2	3	2	1	43.18
16	2	3	1	3	2	3	1	2	46.86
17	2	3	2	1	3	1	2	3	39.18
18	2	3	3	2	1	2	3	1	41.90

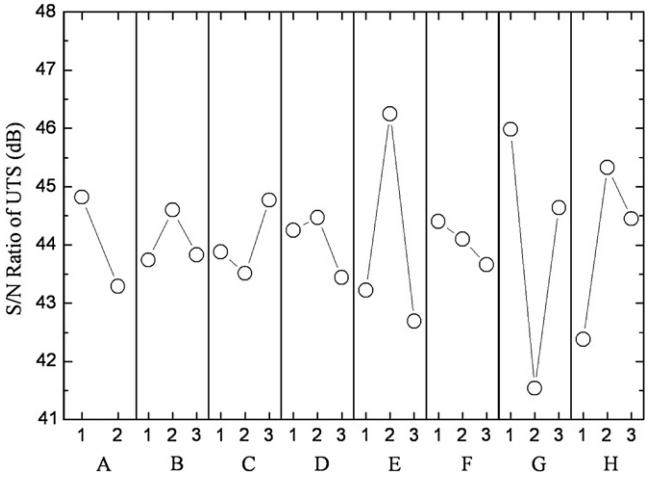

Fig. 1. Corresponding curves of each parameter for EBW of AZ-series alloys.

3. Results and discussion

3.1. Analysis of chemical composition

The chemical compositions of AZ31B, AZ61A, and AZ91D magnesium alloys were analyzed using inductively coupled plasma – atom emission spectrometer and mass spectrometer (ICP-AES and ICP-MS). In Table 2, all of the chemical elements contents meet ASTM standard specifications.

3.2. Taguchi's method for EBW

To explore the trends and contributions of EBW parameters for magnesium alloys, all parameters were subsumed in an $L_{18}(2^1 \times 3^7)$ orthogonal array. After a series of calculations using an HB criterion, the signal-to-noise (S/N) ratio η (units dB) were obtained from the ultimate tensile strength (UTS) of weldment, as Table 3 indicates. Table 4 shows the response list generated by this routine based on Taguchi's method, and Fig. 1 plots the corresponding curves to illustrate the tendency of each parameter. Compared with previous research results [12], no stress relief (A), a focal position at the bottom (E), and a zero oscillation frequency (G) are the same and best choices. Because the oscillation frequency and radius (F) are complementary to each other, no effect will exist if either one is zero; in other words, a zero oscillation frequency can directly represent a non-oscillating beam. However, the accelerating voltage (B), beam current (C), and welding speed (D), exhibit some differences. These differences arise because the individual results of AZ31B, AZ61A, and AZ91D are combined to form integral results. Regarding the difference of material, which is a new parameter in this paper, indicates that AZ61A is the most stable of all three weldments, followed by AZ91D and then AZ31B.

According to the analysis results of variance and contribution shown in Table 5, the oscillation beam contribution (oscillation frequency + oscillation radius ≅ 41%) and focal position (about 29%) are primary parameters which have the most significant effect on AZ-series weldment strength. The reason for this is that magnesium alloy has a much lower liquidus temperature than other engineering materials, such as steel and titanium alloy. Even if the melting point of aluminum alloy approaches that of magnesium alloy, the latter still possesses a lower viscosity than the former under constant input energy conditions. Once under an electron beam with high energy density, the melting magnesium alloy rapidly increases its fluidity as the temperature increases. Not only can the oscillation beam significantly change the weld pool convection to produce many defects, but spatter also occurs easily on the weld surface when the focal position of the electron beam is close to the work piece surface. For the reasons stated above, the oscillation beam's function is not applicable to EBW of magnesium alloy. Using a slightly defocused beam can help to create sound welds, but the electron beam cannot penetrate the work piece as the focal position is excessively downward. Forming various defects after solidification, such areas cause severe stress concentration and reduce the weldment strength [8–11].

Stress relief and material differences are minor factors, with contribution of about 14 and 10%, respectively. When stress relief is not necessary, this indicates that the probability of a crack occurring after welding is very low. On the other hand, the order of AZ-series weldments shows their weldability [11], which is related to the narrowed heat-affected zone and the precipitation of submicron-sized crystals [22]. Additionally, experimental results demonstrate that acceleration voltage, beam current, and welding speed (with contributions of about 2, 3, and 2%, respectively) are fine adjusting factors which should be matched

Table 4
Response list of the levels of all factors for EBW of AZ-series alloys

Level	Parameter							
	A	B	C	D	E	F	G	H
1	44.82	43.74	43.88	44.25	43.22	44.40	45.98	42.38
2	43.29	44.60	43.51	44.47	46.25	44.10	41.54	45.33
3	–	43.83	44.77	43.44	42.69	43.66	44.64	44.45
Robustness	1.53	0.86	1.26	1.03	3.56	0.74	4.44	2.95

Table 5
ANOVA and contribution of parameters for EBW of AZ-series alloys

Parameter (A)	Degree (f_A)	Square sum (S_A)	Variance (V_A)	Contribution (%)
A	1	10.5995	10.5995	13.7396
B	2	2.7160	1.3580	1.7603
C	2	5.0326	2.5163	3.2618
D	2	3.5153	1.7577	2.2784
E	2	44.0271	22.0135	28.5350
F	2	1.7042	0.8521	1.1045
G	2	62.3108	31.1554	40.3851
H	4	27.5733	6.8933	8.9354
Total	17	157.4789	77.1459	–

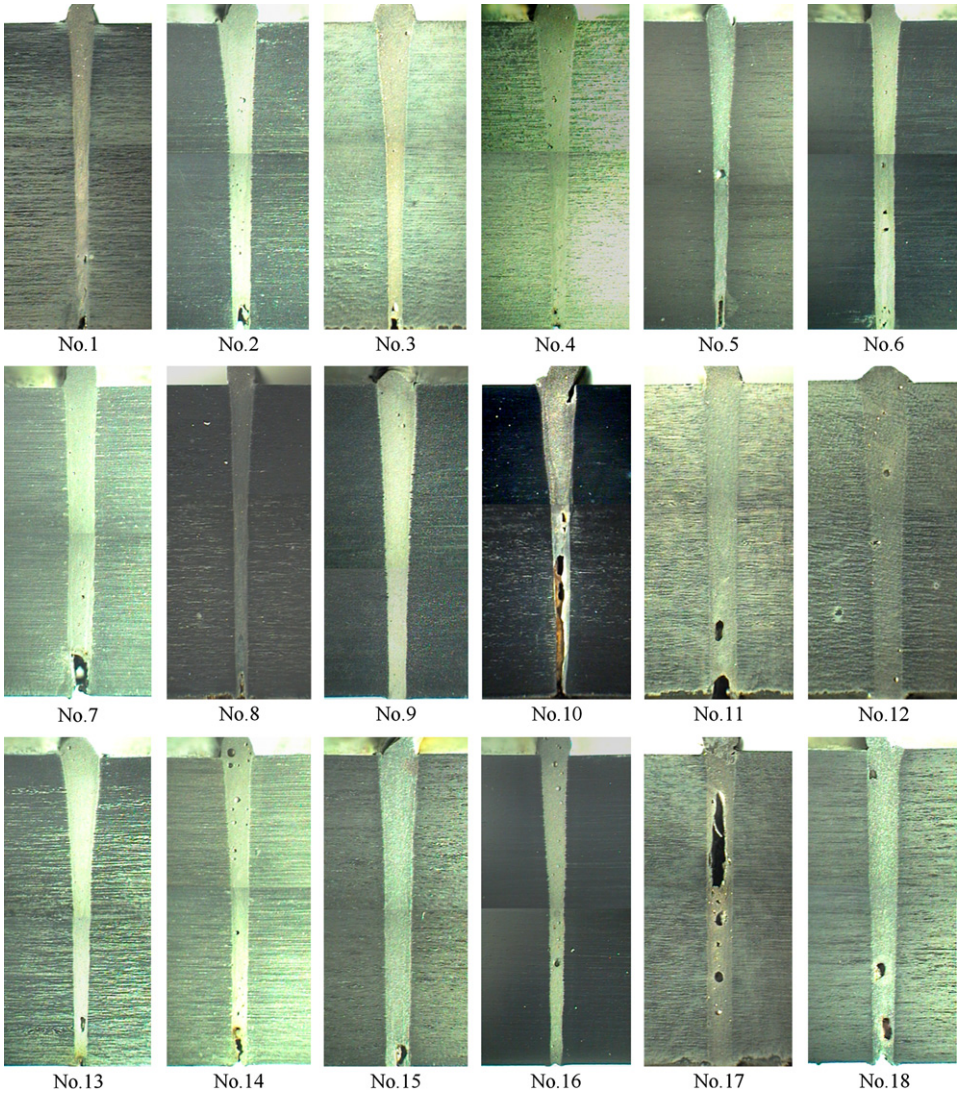

Fig. 2. Metallographic photographs of weld cross-section for 18 sets of experimental runs of Taguchi's method.

Table 6
Measured results of weld defects for EBW of AZ-series alloys

No.	Undercut			Root concavity			Crack or cavity			Pore	
	W_{sur}	D_d	θ_t	W_{sur}	D_d	θ_t	W_{ave}	L_{tol}	θ_t	N_p	R_{ave}
1	0.0	0.0	180.0	328.4	519.4	66.5	0.0	0.0	180.0	10	44.7
2	0.0	0.0	180.0	477.5	831.2	80.4	79.4	412.2	13.2	20	48.6
3	0.0	0.0	180.0	319.6	407.8	78.9	213.6	308.8	58.1	13	52.8
4	0.0	0.0	180.0	317.8	194.2	58.8	0.0	0.0	180.0	22	54.5
5	176.0	123.2	70.8	211.2	1056.0	90.0	0.0	0.0	180.0	2	105.6
6	0.0	0.0	180.0	158.4	123.8	63.6	0.0	0.0	180.0	13	58.0
7	0.0	0.0	180.0	573.0	1443.8	79.2	0.0	0.0	180.0	14	49.1
8	0.0	0.0	180.0	200.6	767.3	50.4	0.0	0.0	180.0	8	37.5
9	108.0	72.0	69.2	0.0	0.0	180.0	0.0	0.0	180.0	0	0.0
10	157.5	740.0	56.5	247.4	4918.7	84.9	78.7	517.4	45.8	6	33.5
11	0.0	0.0	180.0	649.1	669.9	112.1	263.1	784.0	79.6	4	47.8
12	0.0	0.0	180.0	0.0	0.0	180.0	0.0	0.0	180.0	13	69.7
13	0.0	0.0	180.0	176.0	211.2	33.7	158.3	545.6	68.0	12	38.9
14	0.0	0.0	180.0	372.0	1417.2	35.0	0.0	0.0	180.0	18	62.2
15	0.0	0.0	180.0	329.8	789.1	83.7	0.0	0.0	180.0	0	0.0
16	0.0	0.0	180.0	250.5	79.7	108.3	0.0	0.0	180.0	18	64.9
17	0.0	0.0	180.0	0.0	0.0	180.0	364.3	3845.9	21.2	21	62.6
18	0.0	0.0	180.0	532.3	319.4	82.2	214.1	1931.3	23.9	0	0.0

Note 1: W_{sur}, D_d and W_{ave}, L_{tol} are the width, depth of surface concave and the mean width, total length of crack or cavity, respectively (unit: μm). R_{ave} is the mean radius (unit: μm) of pore. θ_t is the tip angle of defect ($0^\circ \le \theta_t \le 180^\circ$). N_p is the number of pores.
Note 2: Quality characteristics of defect dimensions are LB except for θ_t angle (HB).

with each other to form an electron beam with symmetrical Gaussian distribution.

3.3. Grey relational analysis for EBW

Though the influence of EBW parameter on weldment strength can be determined by Taguchi's method, there is not enough evidence to indicate the cause of weld defects. To explain the relationship between EBW parameters and weld defects, grey relational analysis must be applied further. According to previous research results [12,22], the influence of the heat-affected zone on high voltage EBW of AZ-series alloys is very limited, and can therefore be omitted. Weld defects may be classified into four types based on shape, position, and area (i.e. divide defects by calculating the defect area with the same formula). These types include undercut, root concavity, crack or cavity, and pore, and classifying them allows all measured data to be subsumed under the grey relational analysis calculating mode.

Fig. 2 shows metallographic photographs of weld cross-section for the 18 sets of weldments in this study. Table 6 shows the dimensions of all defects as measured by computer software. Because it is very difficult to determine which dimension is more important, each dimensional weight in an individual defect can be obtained by the entropy method after normalizing all measured data, as Table 7

Table 7
Normalized data of weld defects for EBW of AZ-series alloys

No.	Undercut			Root concavity			Crack or cavity			Pore	
	W_{sur}	D_d	θ_t	W_{sur}	D_d	θ_t	W_{ave}	L_{tol}	θ_t	N_p	R_{ave}
1	1.000	1.000	1.000	0.494	0.894	0.369	1.000	1.000	1.000	0.545	0.577
2	1.000	1.000	1.000	0.264	0.831	0.447	0.782	0.893	0.073	0.091	0.540
3	1.000	1.000	1.000	0.508	0.917	0.438	0.414	0.920	0.323	0.409	0.500
4	1.000	1.000	1.000	0.510	0.961	0.327	1.000	1.000	1.000	0.000	0.484
5	0.000	0.834	0.393	0.675	0.785	0.500	1.000	1.000	1.000	0.909	0.000
6	1.000	1.000	1.000	0.756	0.975	0.353	1.000	1.000	1.000	0.409	0.451
7	1.000	1.000	1.000	0.117	0.706	0.440	1.000	1.000	1.000	0.364	0.535
8	1.000	1.000	1.000	0.691	0.844	0.280	1.000	1.000	1.000	0.636	0.645
9	0.386	0.903	0.384	1.000	1.000	1.000	1.000	1.000	1.000	1.000	1.000
10	0.105	0.000	0.314	0.619	0.000	0.472	0.784	0.865	0.254	0.727	0.683
11	1.000	1.000	1.000	0.000	0.864	0.623	0.278	0.796	0.442	0.818	0.547
12	1.000	1.000	1.000	1.000	1.000	1.000	1.000	1.000	1.000	0.409	0.340
13	1.000	1.000	1.000	0.729	0.957	0.187	0.565	0.858	0.378	0.455	0.632
14	1.000	1.000	1.000	0.427	0.712	0.194	1.000	1.000	1.000	0.182	0.411
15	1.000	1.000	1.000	0.492	0.840	0.465	1.000	1.000	1.000	1.000	1.000
16	1.000	1.000	1.000	0.614	0.984	0.602	1.000	1.000	1.000	0.182	0.385
17	1.000	1.000	1.000	1.000	1.000	1.000	0.000	0.000	0.118	0.045	0.407
18	1.000	1.000	1.000	0.180	0.935	0.457	0.412	0.498	0.133	1.000	1.000
ω_{ei}	0.329	0.336	0.335	0.326	0.345	0.329	0.335	0.343	0.322	0.492	0.508

shows. This routine generates the grey relational grade (γ) for each defect based on the grey analysis in Table 8, and then integrates the four sets of γ values into a terminal grey relational grade (γ^*) in the same way. Each defect weight must be adjusted to match the order of the terminal grey relational grade with that of weldment strength, and the grey marks in Table 9 display the experimental runs with coincidental order. Further plotting of this data reveals that both curves possess similar trends found in Fig. 3. Because some interaction exists between all parameters and various defects are randomly distributed in the welds, seriation for the terminal grey relational grade and weldment strength is very difficult to match completely.

From the viewpoint of each defect weight, crack and cavity has the most significant influence on weldment strength (46%), followed by undercut or root concavity (22% each), and then pore (10%). Table 10 shows the relationship between EBW parameters and weld defects after the defect weights were multiplied individually by the contribution of each EBW parameter. This approach clearly reveals that the formative probability of cavity (or crack) with an oscillating beam can reach 19%, and that with a focal position is about 13%, etc. To further understand the EBW parameter and defect shape relationship, it is only necessary to multiply each data point in Table 10 by each dimensional weight in Table 7. This paper does not list these products in detail because the dimensional weights of each defect approximate each other.

Table 8
Grey relational analysis of weld defects for EBW of AZ-series alloys

No.	Grey relational grade for each defect				Total grey relational grade (γ^*)
	Undercut	Root concavity	Crack or cavity	Pore	
1	1.000	0.694	1.000	0.699	0.885
2	1.000	0.665	0.704	0.599	0.768
3	1.000	0.713	0.691	0.651	0.776
4	1.000	0.699	1.000	0.574	0.874
5	0.597	0.730	1.000	0.648	0.817
6	1.000	0.747	1.000	0.641	0.892
7	1.000	0.627	1.000	0.649	0.865
8	1.000	0.699	1.000	0.739	0.890
9	0.653	1.000	1.000	1.000	0.922
10	0.511	0.602	0.731	0.775	0.712
11	1.000	0.663	0.670	0.761	0.769
12	1.000	1.000	1.000	0.619	0.954
13	1.000	0.706	0.715	0.691	0.785
14	1.000	0.628	1.000	0.592	0.860
15	1.000	0.703	1.000	1.000	0.918
16	1.000	0.780	1.000	0.587	0.894
17	1.000	1.000	0.511	0.569	0.767
18	1.000	0.670	0.605	1.000	0.769
ω_i	0.22	0.22	0.46	0.10	–

Table 9
Comparison of the order for 18 sets of experimental runs between weldment strength and weld defect

No. (UTS)	S/N ratio of UTS (dB)	No. γ^*	γ^*
12	48.558	12	0.9541
9	47.816	9	0.9219
4	47.794	15	0.9180
16	46.856	16	0.8942
2	45.787	6	0.8919
13	45.750	8	0.8901
8	45.302	1	0.8849
14	45.050	4	0.8740
1	44.712	7	0.8648
3	44.245	14	0.8597
15	43.176	5	0.8169
6	42.930	13	0.7853
5	42.910	3	0.7763
11	42.846	11	0.7692
18	41.904	18	0.7687
7	41.903	2	0.7677
17	39.176	17	0.7667
10	36.271	10	0.7118

4. Conclusions

The parameters for EBW of AZ-series magnesium alloys may be ranked in order of decreasing influence as follows: beam oscillation, focal position, stress relief, material difference, beam current, welding speed, and accelerating voltage. A non-oscillating beam, a focus at the bottom, and no stress relief are generally the best choices. Weldability follows the order of AZ61A, AZ91D, AZ31B, as determined by the distribution of precipitates and defects. Welding speed, accelerating voltage, and beam current are used to form an electron beam with symmetrical Gaussian distribution, which possesses fine adjusting functions.

Grey relational analysis can effectively integrate various performance characteristics into a system. This analysis reveals that the harmful extent of weld defects follows the order of crack (and cavity), undercut (or root concavity), and pore. The influence of each EBW parameter on various defects is obtained by multiplying defect weight and parameter contribution together. Further, the

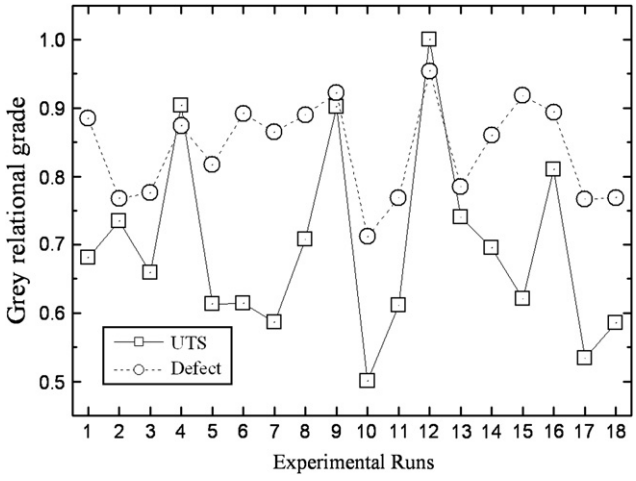

Fig. 3. Curves of grey relational analysis with weldment strength versus weld defect for 18 sets of experimental run of Taguchi's method.

Table 10
Influence of EBW parameters on various weld defects

Parameter	Defect (%)			
	Undercut (22%)	Root concavity (22%)	Crack or cavity (46%)	Pore (10%)
Stress relief (13.7%)	3.0	3.0	6.3	1.4
Accelerating voltage (1.8%)	0.4	0.4	0.8	0.2
Beam current (3.3%)	0.7	0.7	1.5	0.3
Welding speed (2.3%)	0.5	0.5	1.1	0.2
Focal position (28.5%)	6.3	6.3	13.1	2.9
Radius of oscillated EB (1.1%)	0.2	0.2	0.5	0.1
Frequency of oscillated EB (40.4%)	8.9	8.9	18.6	4.0
Difference of material (8.9%)	2.0	2.0	4.1	0.9

influence of each EBW parameter on defect shape can be understood by multiplying the data by dimensional weight.

Acknowledgement

The authors would like to thank M. D. Que of Missile and Rocket Systems Research Division in Chung-Shan Institute of Science and Technology for technical assistance.

References

[1] Schultz DH. Electron beam welding. Cambridge, UK: Abington Hall; 2003.
[2] Lancaster JF. Metallurgy of welding. 5th ed. London, UK: Chapman and Hall; 1993. p. 85.
[3] Petrov P, Georgiev C, Petrov G. Vacuum 1998;51(3):339–43.
[4] Laflamme GR, Powers DE. Weld J 1991:33–40.
[5] Dilthey U, Weiser J. Weld World 1997;39(2):89–98.
[6] Hashimoto T, Matsuda F. Trans Natl Res Inst Met 1965;7(5):12–20.
[7] Koleva E. Vacuum 2005;77:413–21.
[8] Chi CT, Chao CG, Huang CA, Lee CH. Mater Sci Forum 2006;505–507: 193–8.
[9] Chi CT, Chao CGJ. Mater Process Technol 2006;182(1–3):369–73.
[10] Chi CT, Chao CG, Liu TF, Wang CC. Mater Sci Eng 2006;435–436A:672–80.
[11] Chi CT, Chao CG. Weld J 2007;86(5):113s–8s.
[12] Chi CT, Chao CG, Liu TF, Wang CC. Sci. Technol. Weld. Join, in press.
[13] Deng JL. Syst Control Lett 1982;5:288–94.
[14] Deng JL. J Grey Syst 1989;1(1):1–24.
[15] Lin JL, Lin CL. Int J Mach Tool Manuf 2002;42:237–44.
[16] Pan LK, Wang CC, Wei SL, Sher HF. J Mater Process Technol 2007;182: 107–16.
[17] Pan LK, Wang CC, Shin YC, Sher HF. Sci Technol Weld Joining 2005;10(4): 1–8.
[18] Peace GS. Taguchi methods: a hands-on approach. Massachusetts, USA: Addison-Wesley; 1993.
[19] Pan LK, Wang CC, Hsiao YC, Ho KC. Opt Laser Technol 2004;37:33–42.
[20] Kuo HC, Wu LJ. J Mater Process Technol 2002;120:151–68.
[21] ASTM B557-02. 2002. 1–15.
[22] Chi CT, Chao CG, Liu TF, Lee CH. Scr Mater 2007;56(9):733–6.